

Measurement of the F -Meson Lifetime

C. Jung, S. Abachi, C. Akerlof, P. Baringer, I. Beltrami, D. Blockus, G. Bonvicini, B. Brabson, J. M. Brom, B. G. Bylsma, J. Chapman, B. Cork, R. DeBonte, M. Derrick, D. Errede, K. K. Gan, S. W. Gray, J.-P. Guillaud, N. Harnew, P. Kesten, D. Koltick, P. Kooijman, F. J. Loeffler, J. S. Loos, E. H. Low, R. L. McIlwain, D. I. Meyer, D. H. Miller, B. Musgrave, H. Neal, C. R. Ng, D. Nitz, H. Ogren, L. E. Price, L. K. Rangan, J. Repond, D. R. Rust, J. Schlereth, E. I. Shibata, K. Sugano, R. Thun, T. Trinko, M. Valdata-Nappi, J. M. Weiss, M. Willutzky, and D. E. Wood
(The HRS Collaboration)

Indiana University, Bloomington, Indiana 47405

Argonne National Laboratory, Argonne, Illinois 60439

University of Michigan, Ann Arbor, Michigan 48109

Purdue University, West Lafayette, Indiana 47907

Lawrence Berkeley Laboratory, Berkeley, California 94720

(Received 3 January 1986)

The lifetime of the F^\pm meson has been measured to be $(3.5^{+2.4}_{-1.8} \pm 0.9) \times 10^{-13}$ s by means of the $F^\pm \rightarrow \phi\pi^\pm$ decay mode. The measurement was made with the High Resolution Spectrometer at the SLAC e^+e^- storage ring PEP at a center-of-mass energy of 29 GeV.

PACS numbers: 13.25.+m, 14.40.Jz

In this Letter, we report the first measurement of the lifetime of $F^\pm(1970)$ mesons¹ produced in e^+e^- annihilations and decaying into $\phi\pi^+$. The observation of the decay mode $F^+ \rightarrow \phi\pi^+$ in e^+e^- annihilations was reported by Chen *et al.*² and subsequently confirmed by several other experiments.³⁻⁵ The only information on the lifetime of the F^+ meson, however, has come from two fixed-target experiments, one using nuclear emulsions⁶ and the other using a silicon strip detector.⁷ The measurement reported here was made using a high-precision straw-type drift chamber together with the High Resolution Spectrometer (HRS) at the SLAC e^+e^- storage ring PEP. The excellent mass resolution of this detector provides a sample of F^+ candidates with little background.

The lifetime of the F^+ meson is of special interest because of the large difference in the lifetimes of the D^0 and the D^+ mesons. Models explaining this difference include those which emphasize the enhancement of the D^0 decay rate due to a significant contribution from a W -exchange diagram, and those emphasizing the suppression of the D^+ decay rate due to the destructive interference between the two spectator diagrams in the Cabibbo-angle-allowed decays. These models, however, have not yet given satisfactory agreement with measurements.⁸ The principal decay diagrams of the F^+ meson are similar to those of the D^0 meson, except for replacement of the W -exchange diagram with an annihilation diagram. The measurement of the lifetime of the F^+ meson should be valuable in helping to sort out the possible explanations.

The data used in this analysis correspond to an integrated luminosity of 145 pb^{-1} obtained with the HRS detector at the PEP storage ring, at a center-of-mass energy of 29 GeV. A general description of the

detector can be found elsewhere.⁹

The tracking systems of the detector are especially important for this analysis. The outer drift chamber, which consists of two cylindrical layers of drift tubes, is located 1.9 m from the beam axis. The central drift chamber has fifteen cylindrical layers of sense wires at radii between 0.2 and 1.1 m. There are seven axial layers and eight stereo layers with stereo angles of ± 60 mrad relative to the beam axis. Both chambers have an intrinsic resolution of less than $200 \mu\text{m}$. The straw-type vertex chamber, which has operated at HRS since 1983, consists of four cylindrical layers of aluminized Mylar tubes. Each tube is 0.007 m in diameter and 0.4 m long. The innermost layer of the vertex chamber is located at 0.09 m from the beam axis while the outermost layer is at 0.11 m. There are 352 tubes, each with an intrinsic resolution of about $100 \mu\text{m}$. The efficiency of each layer exceeds 99% after an 8% correction for the dead space between tubes. The material in the vertex chamber corresponds to 0.4% of a radiation length. All three chambers operate inside a solenoidal magnetic field of 1.62 T.

The relative alignment of the three tracking elements is critically important in optimization of the resolution of the detector. The vertex chamber and the outer drift chamber were aligned with respect to the central drift chamber system by use of Bhabha events. In addition, a wire-by-wire alignment was performed on the vertex chamber system using the same events. The chambers were realigned for each running cycle which consists of several months of data. Checks of the alignment were made by use of muon pair tracks.

The sample of F^+ mesons was obtained by our ob-

serving the decay mode of $F^+ \rightarrow \phi\pi^+$. The ϕ -meson candidates were selected by our forming combinations from all pairs of oppositely charged particles each interpreted as a kaon and each having a momentum greater than 500 MeV/c. The K^+K^- invariant mass was required to be within ± 10 MeV/ c^2 of 1019.6 MeV/ c^2 . To reduce the combinatorial background, a one-constraint kinematic fit was performed on the track parameters of the two-kaon system subject to a ϕ mass constraint. After rejection of events with χ^2 greater than sixteen in this fit, 49% of the total ϕ sample remained. These events were then combined with all the other charged particles and required to have a $z_{\phi\pi} > 0.4$.¹⁰ To enhance the signal-to-background ratio further, decay-angle cuts were applied that favor the decays of the spin-1 ϕ and the spin-0 F^+ in the decay mode $F^+ \rightarrow \phi\pi^+$. The requirements were $|\cos(\theta_k)^*| > 0.5$ in the ϕ system, and $|\cos(\theta_\phi)^*| < 0.9$ in the F^+ system.¹¹ Further details of the event-selection criteria can be found in a previous publication.³

The following method was used to measure the F^+ lifetime.¹² The decay distance was determined for each event by use of the average beam position, the decay-vertex position of the F^+ candidate, the associated error matrices, and the dip angle of the F^+ flight direction. The decay distances were converted to proper decay times by use of the measured momentum of each F^+ candidate. The average beam position in the plane perpendicular to the e^+ and e^- beams was obtained by a fitting of the track parameters of an ensemble of all the high-quality Bhabha tracks for each run period. Typically, a run lasted one to two hours and yielded an integrated luminosity of approximately 100 nb⁻¹. With use of the impact-parameter distributions for these Bhabha tracks the beam sizes were measured to be 385 ± 10 μ m horizontally and 95 ± 10 μ m vertically. In addition to the physical beam size, these values reflect small contributions from the movement of the beams during a run, and other second-order errors which come mainly from wire sag and misalignment.

The F^+ -decay-vertex resolution depends strongly on the opening angles between the track pairs and on the quality of the tracks. Tracks used in the vertex fit were required to have at least three measured points in the vertex-chamber layers and not to share those points with any other track in order to prevent possible distortion of the track trajectories. Events in which two or more tracks from the F^+ decay were of low quality were rejected. These requirements reduced the event sample by 35%. Since the two kaon tracks from ϕ decay at PEP energies are almost parallel in the vicinity of the decay point, we chose that kaon track with the better quality, together with the pion track, to determine the F^+ -decay-vertex position. From the

parameters of these two tracks, the decay-vertex position in the plane perpendicular to the beams was determined with a χ^2 -minimization technique.

Some additional events were rejected on the basis of the quality of this decay-vertex fit. The error in the fitted decay-vertex position in the plane perpendicular to the beams was required to be less than 1.2 mm along the F^+ flight direction. This requirement reduced the event sample by an additional 10%.

The resulting $\phi\pi$ invariant-mass plot of the final event sample is shown in Fig. 1. A narrow peak with a full width of 20 MeV/ c^2 is seen at 1964 MeV/ c^2 . Three mass ranges were selected for further analysis: the lower background region (1.70 GeV/ $c^2 < m_{\phi\pi} < 1.91$ GeV/ c^2), the F^+ signal region (1.94 GeV/ $c^2 < m_{\phi\pi} < 1.99$ GeV/ c^2), and the upper background region (2.03 GeV/ $c^2 < m_{\phi\pi} < 2.30$ GeV/ c^2). The seventeen events which were observed in the F^+ signal region were used for the F^+ lifetime measurement.

The most probable decay distance in the plane perpendicular to the beams was calculated for each F^+ candidate by use of the expression¹³

$$l' = \frac{x_v \sigma_{yy} t_x + y_v \sigma_{xx} t_y - \sigma_{xy} (x_v t_y + y_v t_x)}{\sigma_{yy} t_x^2 + \sigma_{xx} t_y^2 - 2\sigma_{xy} t_x t_y},$$

where (x_v, y_v) is the decay-vertex position relative to the average beam position, the σ_{ij} are the sum of the decay vertex and beam error matrices, and the t_i are the two-dimensional direction cosines. The full three-dimensional decay distance was obtained from l' by use of the relation $l = l'/\sin\theta$, where θ is the polar angle of the F^+ flight direction. The resulting proper decay time distribution is shown in Fig. 2(a) for the F^+ signal region. The probability that this distribution resulted from the random fluctuation of zero lifetime is about 2%. The associated error in the proper decay

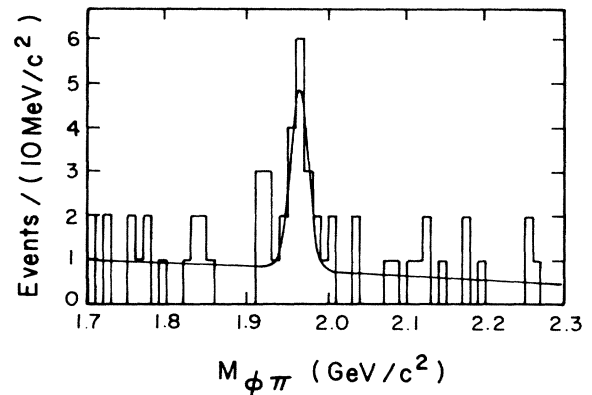


FIG. 1. Invariant-mass plot of $\phi\pi$ combinations showing the F^+ peak at 1964 MeV/ c^2 with a full width of 20 MeV/ c^2 . The curve is a Gaussian plus a flat background.

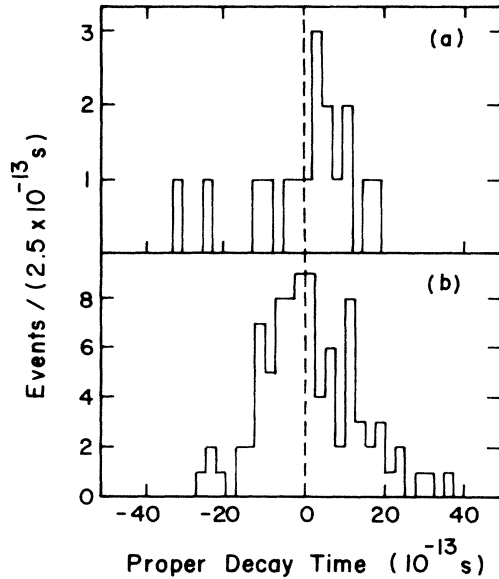


FIG. 2. (a) Proper-decay-time distribution of the seventeen events in the F^+ signal region, $1.94 \text{ GeV}/c^2 < m_{\phi\pi} < 1.99 \text{ GeV}/c^2$, in Fig. 1. (b) Proper-decay-time distribution of the 88 events in the background regions without the decay-angle cuts.

time of each event ranges from $(3 \text{ to } 15) \times 10^{-13} \text{ s}$ and peaks at about $8 \times 10^{-13} \text{ s}$.

A maximum-likelihood fit was used to extract the proper lifetime. The resulting lifetime of the F^+ meson is $(3.5_{-1.8}^{+2.4}) \times 10^{-13} \text{ s}$ (statistical errors only). The contribution of B meson decay to the F^+ with $z_{F^+} > 0.4$ was taken to be 8%,¹⁴ and the current world average value of 1.1 ps was used as the B lifetime. The fraction of the combinatorial background in the F^+ signal region was determined to be 24%. To extract an apparent lifetime of the background, events in the lower and upper background regions were taken without application of the angle cuts in order to increase the statistical sample. There were a total of 88 such events. The resulting proper decay time distribution shown in Fig. 2(b) leads to a background lifetime of $(-0.4 \pm 0.9) \times 10^{-13} \text{ s}$, consistent with zero. A zero-background lifetime was used in the fit for the F^+ lifetime measurement.

The estimate of the systematic error for this analysis is based on the following considerations:

To check for possible bias in the method of determining lifetimes, three sets of hadronic events were simulated by Monte Carlo techniques with the input F^+ lifetimes of $(0, 2, \text{ and } 10) \times 10^{-13} \text{ s}$. The resulting lifetimes were measured to be $(-0.1 \pm 0.6, 3.0 \pm 0.7, \text{ and } 8.7 \pm 1.1) \times 10^{-13} \text{ s}$ (statistical errors only).

The error in the F^+ -decay position depends on the errors which are assigned to the measured track parameters and directly influences the final results of

this analysis. To check whether this error assignment is proper or not, a two-dimensional maximum-likelihood fit was used to determine the most likely error size as well as the lifetime. The fitted errors were found to be within $\pm 5\%$ of the estimated values in both larger samples of data such as D^0 decays and Monte Carlo event samples. The contribution to the systematic error from this source is estimated to be $\pm 0.2 \times 10^{-13} \text{ s}$.

From the uncertainty in the placement of the cut to remove events which fit badly to a common vertex, a contribution of $\pm 0.2 \times 10^{-13} \text{ s}$ systematic error to the lifetime was estimated.

For the estimated uncertainty of 20% in the background fraction, the corresponding lifetime change was $\pm 0.1 \times 10^{-13} \text{ s}$.

Changing of the background lifetime by $1.0 \times 10^{-13} \text{ s}$ yielded a change in the F^+ lifetime of $0.1 \times 10^{-13} \text{ s}$.

Changing of the contribution to the F^+ sample from the B -meson decay by $\pm 8\%$ resulted in a lifetime change of $\mp 0.3 \times 10^{-13} \text{ s}$.

Allowing 50% uncertainty in the B lifetime resulted in a negligible change in the F^+ lifetime.

The contribution from the uncertainties in beam position and beam size to the systematic error is negligible.

A linear sum of all the above contributions gives an estimate for the total systematic error on the measured F^+ meson lifetime of $\pm 0.9 \times 10^{-13} \text{ s}$.

In conclusion, we report a measurement of the F^+ meson lifetime of $\tau_{F^+} = (3.5_{-1.8}^{+2.4} \pm 0.9) \times 10^{-13} \text{ s}$ based on a sample of seventeen $F^+ \rightarrow \phi\pi^+$ decays. Figure 3 shows the results of published F^+ lifetime measurements along with the world average D^0 and D^+ lifetimes.

The techniques used for the three measurements of the F^+ lifetime are quite different. Both of the fixed-target experiments benefit from good vertex resolution which leads to the negligible error in the decay-distance determination. The event selections of these experiments, however, are not completely lifetime independent and have some possibility of contamination from other processes. On the other hand, our measurement is characterized by an event selection which is independent of the lifetime and also by a clean separation of the F^+ signal from background and other processes, although the error in the decay distance is comparable to the decay distance itself. All three measurements agree well and are close to the D^0 lifetime.

We thank the PEP operation group for their continuous effort to provide us with stable beams and good luminosities, and the cryogenics group for maintaining our superconducting magnet in smooth operation. This work was supported in part by the U. S. Department of Energy under Contracts No. W-31-

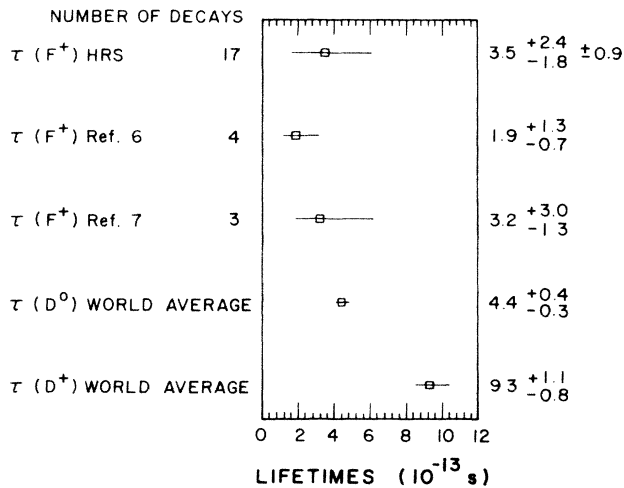


FIG. 3. Comparison of lifetime measurements; τ_{F^+} , τ_{D^0} , and τ_{D^+} . Only statistical errors are quoted for the measurements by the experiments of Refs. 6 and 7.

109-ENG-38, No. DE-AC02-76ER01112, No. DE-AC03-76SF000998, No. DE-AC02-76ER01428, and No. DE-AC02-84ER40125.

¹In this article the F^+ meson will refer to both the F^+ and its antiparticle F^- . The F^+ meson is the $c\bar{s}$ ground state of the $q\bar{q}$ system.

²A. Chen *et al.*, Phys. Rev. Lett. **51**, 634 (1983).

³M. Derrick *et al.*, Phys. Rev. Lett. **54**, 2568 (1985).

⁴H. Albrecht *et al.*, Phys. Lett. **153B**, 343 (1985).

⁵M. Althoff *et al.*, Phys. Lett. **136B**, 130 (1984).

⁶N. Ushida *et al.*, Phys. Rev. Lett. **51**, 2362 (1983).

⁷R. Bailey *et al.*, Phys. Lett. **139B**, 320 (1984).

⁸H.-Y. Cheng, in *Proceedings of the Oregon Meeting*, edited by R. C. Hwa (World Scientific, Singapore, 1986).

⁹D. Bender *et al.*, Phys. Rev. D **30**, 515 (1984).

¹⁰ z is defined as the ratio of particle energy to the beam energy.

¹¹ θ_ϕ is the angle made by the ϕ in the F^+ rest frame with respect to the F^+ in the laboratory frame and θ_K is the angle of the K^+ in the ϕ rest frame with respect to the ϕ in the F^+ rest frame.

¹²To minimize the systematic uncertainty in the measured lifetime, only the information from the vertex chamber and the central drift chamber were used for this part of the analysis.

¹³J. Jaros *et al.*, Phys. Rev. Lett. **51**, 955 (1983).

¹⁴M. Suzuki, Phys. Rev. D **31**, 1158 (1984), and Phys. Lett. **142B**, 305 (1984).